Journal of NeuroVirology, 7: 466–475, 2001
 ISSN 1355–0284/01 $12.00+.00

Enhanced proteolysis of IκBα and IκBβ proteins in astrocytes by Moloney murine leukemia virus (MoMuLV)-*ts*1 infection: A potential mechanism of NF-κB activation

Hun-Taek Kim,[1] Wenan Qiang,[2] Paul KY Wong,[2] and George Stoica[1]

[1]*Department of Veterinary Pathobiology, Texas A&M University, College Station, Texas, USA; and* [2]*Department of Carcinogenesis, The University of Texas, MD Anderson Cancer Center, Science Park-Research Division, Smithville, Texas, USA*

Moloney murine leukemia virus (MoMuLV)-*ts*1-mediated neuronal degeneration in mice is likely due to loss of glial support and release of inflammatory cytokines and neurotoxins from surrounding *ts*1-infected glial cells including astrocytes. NF-κB is a transcription factor that participates in the transcriptional activation of a variety of immune and inflammatory genes. We investigated whether *ts*1 activates NF-κB in astrocytes and examined the mechanism(s) responsible for the activation of NF-κB by *ts*1 infection *in vitro*. Here we present evidence that *ts*1 infection of astrocytes *in vitro* activates NF-κB by enhanced proteolysis of the NF-κB inhibitors, IκBα and IκBβ. In *in vitro* studies using protease inhibitors, IκBα proteolysis in *ts*1-infected astrocytes was significantly blocked by a specific calpain inhibitor calpeptin but not by MG-132, a specific proteasome inhibitor, whereas rapid IκBβ proteolysis was blocked by MG-132. Furthermore, treatment with MG-132 increased levels of multiubiquitinated IκBβ protein in *ts*1-infected astrocytes. These results indicate that the calpain proteolysis is a major mechanism of IκBα proteolysis in *ts*1-infected astrocytes. Additionally, *ts*1 infection of astrocytes *in vitro* increased expression of inducible nitric oxide synthase (iNOS), a NF-κB-dependent gene product. Our results suggest that NF-κB activation in *ts*1-infected astrocytes is mediated by enhanced proteolysis of IκBα and IκBβ through two different proteolytic pathways, the calpain and ubiquitin-proteasome pathways, resulting in increased expression of iNOS, a NF-κB-dependent gene. *Journal of NeuroVirology* (2001) **7,** 466–475.

Keywords: MoMuLV-*ts* 1; NF-κB; IκB; astrocytes; iNOS

Introduction

Moloney murine leukemia virus (MoMuLV), a murine type C retrovirus, induces T-cell lymphoma after a long incubation period in susceptible strains of mice (Gardner, 1978; Peters *et al*, 1973). Its temperature-sensitive mutant *ts* 1, a lymphotropic and neurotropic strain of MoMuLV with a single point mutation in the envelope gene, causes loss of T cells and motor neurons in susceptible hosts (Wong *et al*, 1989; Szurek *et al*, 1990; Wong *et al*, 1991). After exposure to *ts* 1, mice develop a progressive neurodegenerative disease that morphologically manifests as spongiform polioencephalomyelopathy. *ts* 1-mediated neuronal degeneration is likely due to loss of glial support and release of proinflammatory cytokines and neurotoxins from surrounding *ts* 1-infected glial cells, a hypothesis based on several observations. First, *ts* 1 replicates in endothelial, ependymal, and glial cells but not in motor neurons (Stoica *et al*, 1993).

Address correspondence to George Stoica, DVM, PhD, Professor, Department of Veterinary Pathobiology, Texas A&M University, College Station, TX 77843, USA. E-mail: gstoica@cvm.tamu.edu

Received 7 February 2001; revised 10 April 2001; accepted 8 May 2001.

Second, in regions in which *ts*1-infected brain stems are severely affected, expression of tumor necrosis factor-α (TNF-α), interleukin-1 (IL-1), Fas and its ligand increases (Choe *et al*, 1998). Third, as shown in an *in vitro* study, *ts*1 infection in astrocytes either kills or causes astrocytes to differentiate into macrophage-like cells secreting TNF-α and IL-1 late in the period of infection (Wong *et al*, unpublished results).

NF-κB transcription factors play a central role in the regulation of genes implicated in immune and stress responses, inflammation, cell growth control, and apoptosis (Baeuerle and Baltimore, 1996; Baldwin, 1996; Sonenshein, 1997). NF-κB is composed of homo- and heterodimeric complexes of members of the Rel/NF-κB family. The vertebrate Rel/NF-κB family is composed of RelA (p65), p50, c-Rel, p52, and RelB. In most cell types, the majority of NF-κB dimers is sequestered within the cytoplasm in an inactive state. The molecular mechanism responsible for the cytosolic retention of NF-κB involves NF-κB's association with the inhibitory members of the IκB family of proteins (Beg and Baldwin, 1993; Liou and Baltimore, 1993). The IκB family of inhibitors is mainly represented by IκBα and IκBβ but also includes IκBγ, Bcl-3, p105, and p100. In response to a large variety of inducers (e.g., TNF-α, IL-1, and lipopolysaccharide (LPS)), IκBα and IκBβ are rapidly degraded through the ubiquitin-proteasomal pathway (Chen *et al*, 1995; DiDonato *et al*, 1996), which allows NF-κB to translocate into the nucleus and activate the transcription of NF-κB-dependent genes such as TNF-α, IL-2, IL-6, MHC class I, and inducible nitric oxide synthase (iNOS) (Baeuerle and Baltimore, 1996; Baldwin, 1996). NF-κB is also activated by a number of viruses such as herpes virus, human immunodeficiency virus type I (HIV-1), adenovirus, and MoMuLV (Pak and Faller, 1996; Patel *et al*, 1998; Asin *et al*, 1999; Borgland *et al*, 2000). Also, the tax protein of the human T-cell lymphotropic virus type I increases NF-κB DNA-binding activity in cells (McKinsey *et al*, 1996; Rousset *et al*, 1996). HIV-1 infection of the central nervous system (CNS) appears to involve NF-κB, either as a regulator of viral transcription or in viral clearance (Dollard *et al*, 1995; Wu *et al*, 1995); this in turn points to a role for NF-κB in HIV-induced pathological changes in the CNS.

Recent evidence suggests that viruses interact with the ubiquitin-proteasome pathway (Rousset *et al*, 1996). For example, up-regulation of this pathway was apparently involved in a murine immunodeficiency viral infection (Crinelli *et al*, 1997; Crinelli *et al*, 1999). We also reported an increase in the numbers of the neuronal cells showing immunoreactivity to an anti-ubiquitin antibody in *ts*1-induced encephalopathy (Stoica *et al*, 2000). A single amino acid substitution, Val-25-to-Ile in the envelope precursor protein, is responsible for the temperature-sensitive inefficient transport of envelope protein in the endoplasmic reticulum (Szurek *et al*, 1990). This mutation has been correlated with *ts*1's neurovirulence (Szurek *et al*, 1990; Wong *et al*, 1991). In a previous study, we showed that the cytopathic effects of *ts*1 on primary astrocytes *in vitro* closely correlated with the accumulation of *ts*1 precursor envelope protein in the ER (Shikova *et al*, 1993). A recent study identified ER retention of viral proteins as a NF-κB-activating signal (Pahl *et al*, 1996).

We were therefore interested in investigating the activation status of NF-κB in astrocytes by *ts*1 infection and the mechanism(s) responsible for the activation of NF-κB by *ts*1 infection. In the present study, we examined the effects of *ts*1 infection on NF-κB activation in an immortalized astrocyte cell line (called C1 astrocytes) that has been known to develop similar cytopathic effects by *ts*1 infection, as in primary astrocytes (Lin *et al*, 1997). We report that infection of C1 astrocytes by *ts*1 *in vitro* increased the proteolysis of IκBα and IκBβ along two different proteolytic pathways, the calpain and ubiquitin-proteasome pathways, leading to the activation of NF-κB in astrocytes.

Results

ts*1-induced decreases in IκBα and IκBβ proteins in C1 astrocytes*

The time course of Rel/NF-κB and IκB protein expression in C1 astrocytes after *ts*1 infection was determined by immunoblotting using specific antibodies to individual proteins. As shown in Figure 1A, there was no detectable difference in expression of RelA protein between mock-infected and *ts*1-infected C1 astrocytes. The levels of p50 protein slightly increased in *ts*1-infected astrocytes compared with mock-infected controls. There was no change in levels of IκB proteins in mock-infected controls. However, the levels of IκBα and IκBβ proteins in *ts*1-infected astrocytes compared with mock-infected controls decreased over time after infection. *ts*1 infection induced a significant reduction of IκBβ level even at 24 h p.i. ($P < 0.01$); a similar reduction in IκBα level occurred much later (48 or 72 h p.i.) ($P < 0.01$) (Figure 1B). The gradual loss of immunoreactive IκBα protein in *ts*1-infected C1 astrocytes was accompanied by a decrease in the abundance of a slower-migrating band, presumably representing a hyperphosphorylated form of IκBα. In mock-infected controls, there was no change in levels of hyperphosphorylated IκBα proteins that were more abundant compared with those for *ts*1-infected C1 astrocytes.

Correlation between decreased levels of IκBα and IκBβ proteins in ts*1-infected C1 astrocytes and increased nuclear translocation of RelA* in vitro

Analysis of nuclear and cytosolic lysates of mock- and *ts*1-infected C1 astrocytes showed that the

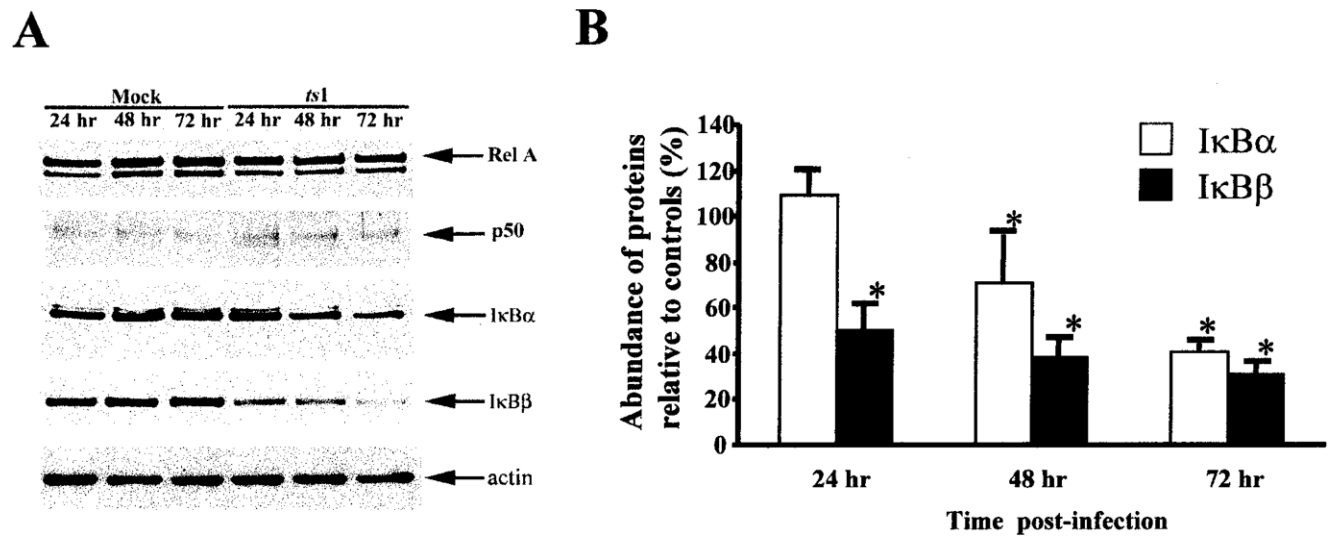

Figure 1 Expression and regulation of Rel/NF-κB and IκB proteins in C1 astrocytes by *ts* 1 infection. (A) Time course of IκBα and IκBβ degradation in C1 astrocytes by *ts* 1 infection. After C1 astrocytes were mock- or *ts* 1-infected, whole cell lysates were prepared at 24, 48, and 72 h p.i. Whole cell lysates (20 μg) were then subjected to Western immunoblotting. (B) Relative decreases in levels of IκBα and IκBβ proteins in *ts*1-infected C1 astrocytes. Protein levels were expressed relative to controls at each time points to compare *ts*1 infection-induced changes in the protein levels using data obtained from densitometric analysis of autoradiographs. The levels of IκBα protein in *ts*1-infected C1 astrocytes were lower than in mock-infected controls at 48 and 72 h ($P < 0.01$); in contrast, the levels of IκBβ protein in *ts*1-infected C1 astrocytes were lower than in mock-infected controls at all time points examined ($P < 0.01$). Results are the means ± standard deviation (SD) from two independent experiments carried out in triplicate ($n = 6$) and are representative of those from two independent experiments.

loss of IκB proteins was associated with increased nuclear translocation of RelA. RelA was predominantly present in the cytoplasm of both mock- and *ts*1-infected C1 astrocytes at 48 h p.i.; however, levels of RelA in the nuclear fraction of *ts*1-infected C1 astrocytes were increased when compared with mock-infected control (Figure 2).

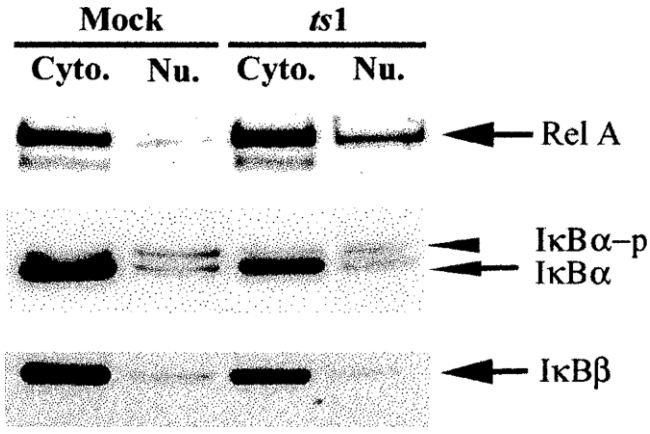

Figure 2 Nuclear translocation of RelA in astrocytes by *ts*1 infection. Nuclear (Nu.) and cytoplasmic (Cyto.) lysates were prepared from mock- and *ts*1-infected C1 astrocytes at 48 h p.i. Nuclear and cytoplasmic extracts (containing 20 μg of protein) were subject to Western immunoblot analyses for RelA, IκBα and IκBβ. The slower-migrating band above IκBα represents a phosphorylated form of IκBα, as indicated by IκBα–p. Results shown are representative of those from three independent experiments.

Two different proteolytic pathways responsible for increased IκBα and IκBβ proteolysis in ts*1-infected C1 astrocytes*

The degradation of IκBα and IκBβ occurs primarily via the ubiquitin-proteasome pathway. However, a number of alternate proteolytic mechanisms for IκBα degradation have recently been described that implicate the calcium-dependent cytosolic protease calpain. Having previously observed that *ts*1 infection selectively decreased levels of IκBα and IκBβ proteins in C1 astrocytes and that the pattern of decrease for IκBα was different from the one for IκBβ, we examined the effects of proteasome and calpain inhibitors on the proteolysis of IκBα and IκBβ in *ts*1-infected C1 astrocytes at 48 h p.i. (Figure 3). The proteolysis of IκBα in *ts*1-infected C1 astrocytes was not efficiently blocked by MG-132, a highly potent proteasome inhibitor, but was significantly blocked by calpeptin, a cell-permeable calpain inhibitor (Figure 3A and 3B). By contrast, IκBβ degradation was effectively blocked by MG-132 but not by calpeptin (Figure 3A and 3B).

To confirm this result, both mock- and *ts*1-infected C1 cells were treated with either MG-132 or calpeptin for another 4 h at 48 and 72 h p.i. MG-132 treatment enhanced the accumulation of a high-molecular-weight ladder representing formation of multiubiquitinated IκBβ proteins in either mock- or *ts*1-infected C1 cells (Figure 3C). Multiubiquitinated IκBβ proteins were more abundant in *ts*1-infected C1 cells treated with MG-132 than in either nontreated *ts*1-infected C1 cells or mock-infected C1 cells treated

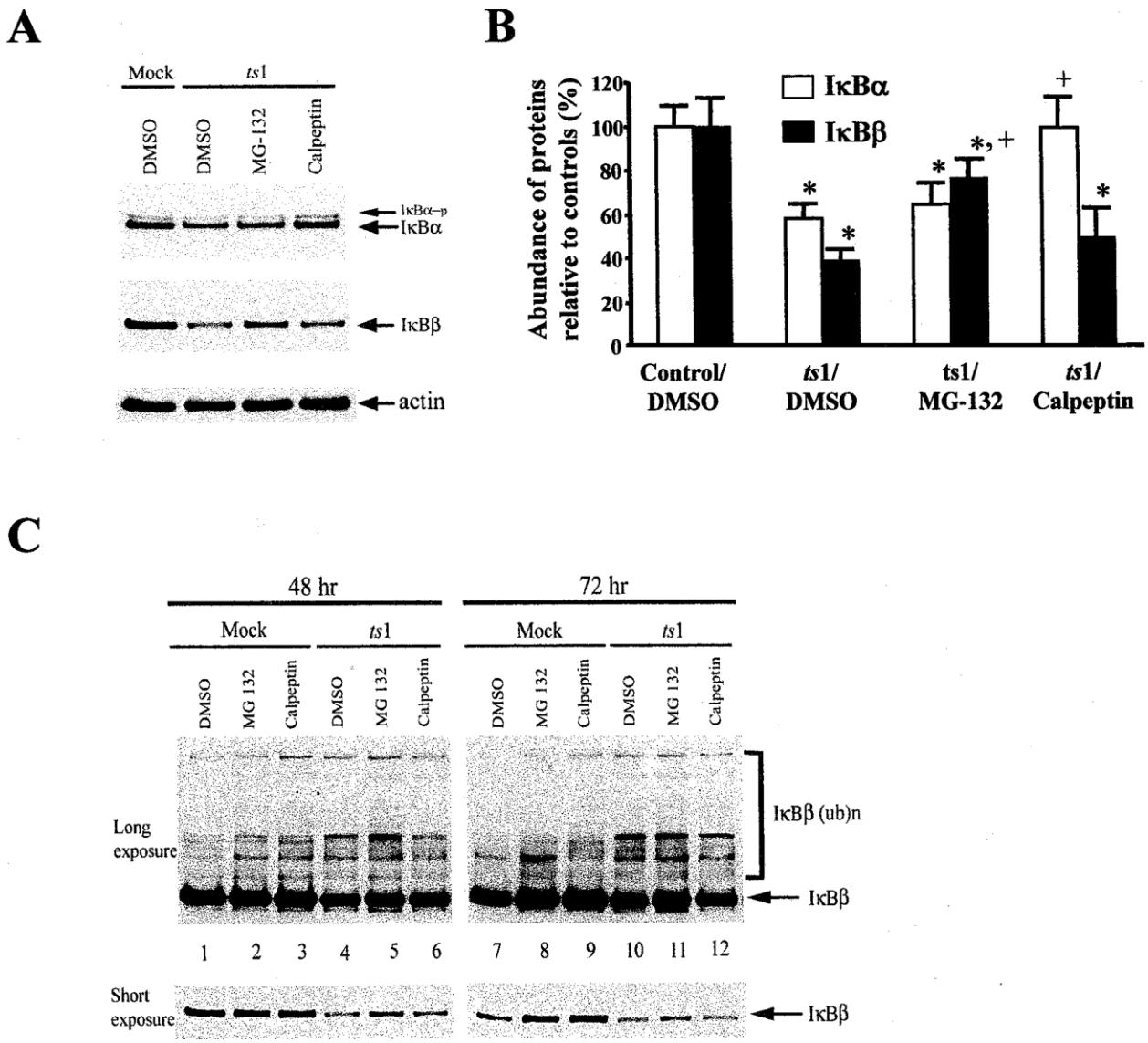

Figure 3 Evidence that different proteolytic pathways are involved in IκBα and IκBβ degradation in *ts*1-infected C1 astrocytes. (A) Effects of calpain and proteasome inhibitors on degradation of IκBα and IκBβ in *ts*1-infected C1 astrocytes. At 48 h p.i., C1 cells were treated with various protease inhibitors for 4 h before cell lysate preparation. Whole cell lysates (20 μg of protein) were then separated by SDS-PAGE and analyzed by Western immunoblotting. The slower-migrating band above IκBα represents a phosphorylated form of IκBα, as indicated by IκBβ–p. (B) Quantitative analysis of levels of IκBα and IκBβ proteins in *ts*1-infected C1 astrocytes after treatment with either calpeptin, MG-132, or dimethyl sulfoxide (DMSO). Protein levels were expressed relative to controls to determine the inhibitory effects of calpeptin and MG-132 on degradation of IκB proteins in C1 astrocytes by *ts*1 infection using data obtained from densitometric analysis of autoradiographs. Results are the means ± SD from three independent experiments carried out in triplicate ($n = 9$) and are representative of those from three independent experiments. *Significantly different from controls ($P < 0.01$). +Significantly different from *ts*1 infection alone (DMSO) ($P < 0.01$). (C) Accumulation of high-molecular-weight ubiquitinated IκBβ forms in the presence of the proteasome inhibitor MG-132. Starting at 48 and 72 h p.i., C1 cells were treated with DMSO, calpeptin, or MG-132 for an additional 4 h before cell lysis preparation. Whole cell lysates (20 μg of protein) were then fractioned by SDS-PAGE and analyzed by Western immunoblotting using a specific anti-IκBβ antibody. Prolonged exposure (upper panels) shows that MG-132 treatment increased levels of high-molecular-weight ubiquitinated IκBβ forms, as indicated by IκBβ (ub)n (compare lanes 4 and 10 with 5 and 11, respectively). Short exposure (lower panels) of anti-IκBβ immunoblots (shown in upper panels) is displayed. Results shown are representative of those from three independent experiments.

with MG-132 at the same time points. Although the levels of IκBβ proteins in *ts*1-infected C1 cells at 72 h p.i. were lower than the levels at earlier time points, the formation of multiubiquitinated IκBβ proteins peaked at 72 h p.i. in *ts*1-infected C1 astrocytes. As expected, calpeptin treatment did not notably produce multiubiquitinated IκBβ proteins in either mock- or *ts*1-infected C1 astrocytes. Also, calpeptin treatment did not induce the accumulation of a high-molecular-weight ladder of IκBα forms

(data not shown). Together, these results provided evidence that different mechanisms were responsible for IκBα and IκBβ proteolysis in *ts*1-infected C1 astrocytes.

Changes in levels of ubiquitin conjugates in C1 astrocytes after ts*1 infection*

To determine whether the ubiquitin-proteasome-mediated increase in IκBβ proteolysis was due to the increase in total ubiquitin conjugation activity, we examined levels of total ubiquitin conjugates in mock- and *ts*1-infected astrocytes at 24, 48, and 72 h p.i. As shown in Figure 4, immunoblotting analysis using a polyclonal anti-ubiquitin antibody revealed that the level of high-molecular-weight ubiquitin conjugates in *ts*1-infected C1 astrocytes were 67 ± 23.4% (mean ± SD) and 44 ± 18.9% higher than those in mock-infected controls at 24 and 48 h p.i. ($P < 0.01$); however, at 72 h p.i., the level of high-molecular-weight ubiquitin conjugates in *ts*1-infected C1 astrocytes had decreased to 78 ± 25.1% of the level in the mock-infected control. There was no observable change in levels of free ubiquitin in mock- and *ts*1-infected astrocytes (data not shown).

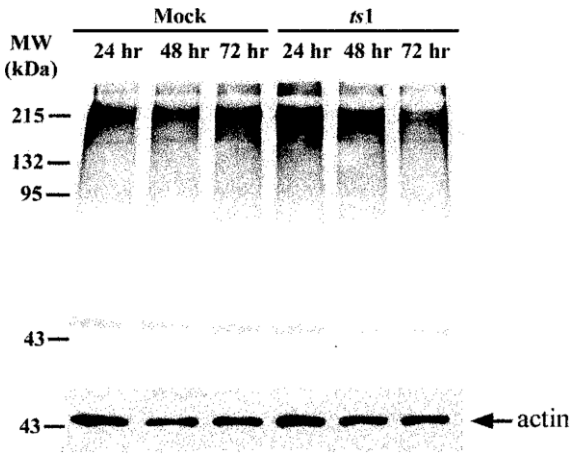

Figure 4 Effects of *ts*1 infection on ubiquitin conjugates in C1 astrocytes. At 24, 48, and 72 h p.i., C1 cells were lysed. Whole cell lysates (containing 20 μg of protein) were then separated by SDS-PAGE and analyzed by Western immunoblotting using a specific anti-ubiquitin antibody. At 24 and 48 h p.i., the levels of high-molecular-weight ubiquitin conjugates in *ts*1-infected C1 astrocytes had significantly increased to 67 ± 23.4% (mean ± SD) and 44 ± 18.9% over those in mock-infected controls ($P < 0.01$), but, by 72 h p.i., had decreased to 78 ± 25.1% of the level in the mock-infected control, as determined by densitometric analysis of autoradiographs. Results shown are representative of those from three independent experiments.

Increased expression of iNOS in ts *1-infected C1 astrocytes*

To ascertain whether an increase in NF-κB-dependent gene expression coincides with enhanced degradation of IκB as well as nuclear translocation of RelA, levels of expression of iNOS protein, a NF-κB-dependent gene product, in mock- and *ts*1-infected C1 astrocytes was determined (Figure 5A). There was no detectable difference in expression of constitutive form of nitric oxide synthase (cNOS) protein between mock-infected control and *ts*1-infected C1 astrocytes. The iNOS protein level in *ts*1-infected C1 astrocytes

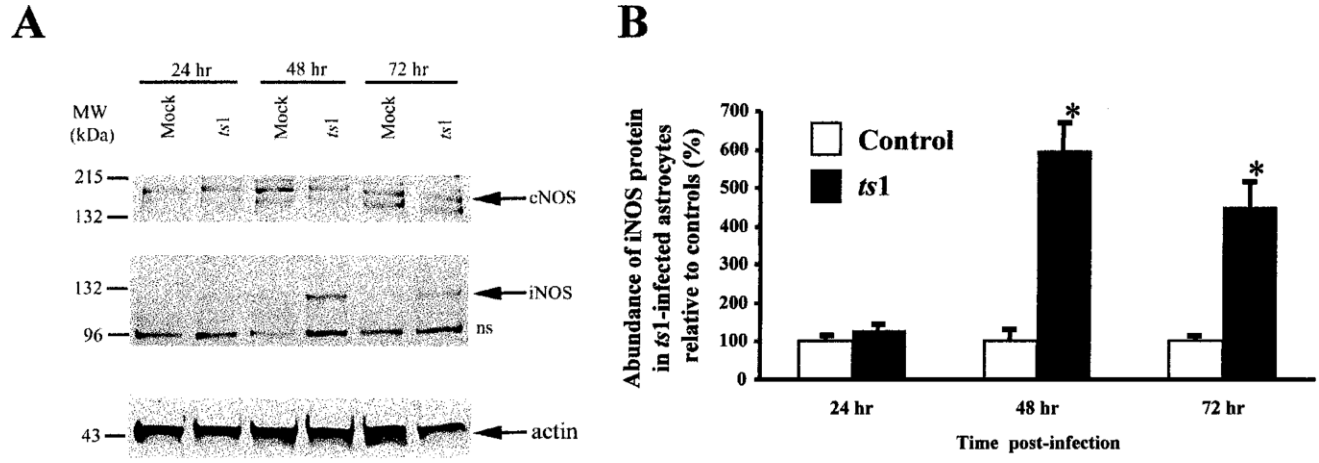

Figure 5 Increased expression of iNOS protein in C1 astrocytes by *ts*1 infection. (A) Time course of levels of cNOS and iNOS proteins in C1 astrocytes by *ts*1 infection. After C1 astrocytes were mock- or *ts*1-infected, whole cell lysates were prepared at 24, 48, and 72 h p.i. Proteins (20 μg/lane) were fractionated by 8% SDS-PAGE and analyzed by Western immunoblotting using either rabbit polyclonal anti-cNOS or -iNOS antibody. Nonspecific bands are shown, as indicated by ns. (B) Relative increases in levels of iNOS proteins in *ts*1-infected C1 astrocytes. Protein levels were expressed relative to controls at each time points to compare *ts*1 infection-induced changes in the protein levels using data obtained from densitometric analysis of autoradiographs. When compared with the levels in mock-infected controls, iNOS protein levels in *ts*1-infected C1 astrocytes increased 5.9- and 4.5-fold by 48 and 72 h p.i. *Significantly different from controls at each time points ($P < 0.01$). Results are the means ± SD from two independent experiments carried out in triplicate ($n = 6$) and are representative of those from two independent experiments.

was slightly higher than that in mock-infected control at 24 h p.i. However, iNOS protein levels in *ts*1-infected C1 astrocytes markedly increased by 48 and 72 h p.i. compared with the levels in mock-infected controls. At 48 and 72 h p.i., iNOS protein levels in *ts*1-infected C1 astrocytes had significantly increased 5.9- and 4.5-fold over those in mock-infected controls (Figure 5B) ($P < 0.01$).

Discussion

Although much is known about the activation of the NFκB transcription factor by extracellular stimuli such as TNF-α and IL-1, comparatively little is known about the mechanisms of NF-κB activation by intracellular stimuli. In the present study, we found evidence that *ts*1, a neurotropic strain of MoMuLV, induces activation of NF-κB in astrocytes. We also showed that at least one of the mechanisms responsible for activation of NF-κB in *ts*1-infected astrocytes is increased degradation of IκBα and IκBβ, two major members of the IκB family.

Several studies have already suggested that phosphorylation- and ubiquitin-dependent degradation of the IκB molecule is a key event for activation of NF-κB (Zandi *et al*, 1997; Hatakeyama *et al*, 1999). Now, our data argue for differences in the proteolysis of IκB proteins in *ts*1-infected astrocytes. Calpeptin, a highly specific calpain inhibitor, was effective in blocking IκBα proteolysis in *ts*1-infected C1 astrocytes, but was not efficiently blocked by MG-132, a highly potent proteasome inhibitor. It should be noted that the concentration of MG-132 used in the present study was sufficient to significantly increase the abundance of total ubiquitin conjugates in either mock- or *ts*1-infected C1 cells, as determined by immunoblotting analysis using an anti-ubiquitin antibody (data not shown), but ineffective at blocking *ts*1-mediated IκBα proteolysis. Thus, it appears that the calpain protease rather than ubiquitin/proteasome pathway is a major effector of IκBα proteolysis in *ts*1-infected astrocytes. This is supported by a recent study showing that IκBα proteolysis induced by respiratory syncytial virus infection occurs independently of the proteasome pathway (Jamaluddin *et al*, 1998), as distinct from the previously reported proteasome-dependent IκBα proteolysis in lymph nodes induced by MuLV (Crinelli *et al*, 1999). However, it should be noted that low-molecular-weight IκBα intermediates (<30 kDa) could be detected only in *ts*1-infected cells treated with MG-132 (data not shown). The appearance of low-molecular-weight forms of IκBα may have been due to inhibition of the further degradation of ~30-kDa IκBα intermediates by MG-132, as demonstrated by another group (Han *et al*, 1999). This in turn suggests that complete IκBα proteolysis may require a combination of calpain and ubiquitin-proteasome pathway. This concept is supported by recent reports that two independent or combined calpain/proteasome pathways are involved in the degradation of various regulatory proteins including IκBα (Han *et al*, 1999; Shirane *et al*, 1999).

The mechanism responsible for the activation of calpain in *ts*1-infected C1 astrocytes remains unknown. *In vitro*, calpains exposed to nonphysiological concentrations of calcium acquire enzymatic activity through autoproteolysis of their constituent subunits (Sorimachi *et al*, 1997). Because HIV envelope proteins have recently been shown to perturb plasma membrane ion transport in astrocytes (Benos *et al*, 1994), it is possible that *ts*1 envelope proteins may interfere with the plasma membrane functions, resulting in a massive influx of calcium and subsequent excessive or uncontrolled calpain activity in *ts*1-infected astrocytes. The mechanism of calpain activation by *ts*1 infection remains to be determined. However, it should be noted that *in vitro* studies do not always reproduce results obtained from *in vivo* studies. Therefore, the biological relevance of our findings from these *in vitro* studies should be confirmed by *in vivo* experiments.

IκBβ degradation differs from that of IκBα. A series of reports have suggested a role for IκBβ reduction in persistent NF-κB activation (Thompson *et al*, 1995; Johnson *et al*, 1996). Also, human T-cell leukemia virus type 1 tax caused activation of NF-κB by increased degradation of IκBβ (Good and Sun, 1996). Our present finding that *ts*1 infection induced more rapid and prominent reduction of IκBβ than IκBα suggests a role for rapid and enhanced IκBβ proteolysis in the activation of NF-κB in C1 astrocytes. It was shown that activated NF-κB stimulates the synthesis of IκBα mRNA but not IκBβ mRNA (Thompson *et al*, 1995), which may explain more slow reduction of levels of IκBα than IκBβ in *ts*1-infected C1 astrocytes.

We tried to explain the mechanism of enhanced IκBβ proteolysis by determining the ubiquitin-conjugating activity. Although the overall ubiquitin-conjugating activity in *ts*1-infected C1 astrocytes was higher than in control early after infection, it declined to levels lower than in controls at 72 h p.i., a time point at which levels of IκBβ protein in *ts*1-infected C1 astrocytes reached a minimum. These results suggest that the increase in proteolysis of IκBβ was not a consequence of the general increase in ubiquitin-conjugating activity in *ts*1-infected C1 astrocytes. One possible explanation for the early increase in ubiquitin-conjugating activity is that cells reacted by modulating or removing the cytopathic injuries induced by *ts*1 infection.

In astrocytes, NO is biosynthesized by the calcium-independent inducible form of NO synthase iNOS, which is normally not present but whose expression is activated by a variety of inflammatory stimuli *in vitro* (Lee *et al*, 1993; Simmons and Murphy, 1993). Astroglial iNOS expression has been described in demyelinating diseases including experimental allergic

encephalomyelitis in rodents (Koprowski *et al*, 1993) and multiple sclerosis in human (Bo *et al*, 1994; Cross *et al*, 1998). The observed induction of iNOS by NFκB activation in *ts*1-infected C1 astrocytes probably results in generation of nitric oxide, a potent inflammatory mediator that induces a neurotoxic oxidative stress on neurons *in vivo* (Akama *et al*, 1998). iNOS is an attractive candidate for mediating NO-associated neurologic damage by *ts*1 infection, because it functions independently of signals that modulate other forms of NO synthase such as cNOS. After induction of iNOS protein, iNOS will produce NO until certain cellular processes remove iNOS protein or the enzymatic substrates are depleted. Thus, a large amount of NO may be produced by iNOS. Whether preventing or reducing iNOS expression can be of therapeutic value in the prevention of neurological damage associated with *ts*1 infection in animal studies remains to be determined.

In conclusion, results of the present study showed that, in *ts*1-infected astrocytes, two different proteolytic pathways, the calpain and ubiquitin-proteasome pathways, are involved in the proteolysis of IκBα and IκBβ, respectively, leading to increase in NF-κB-dependent gene expression.

Materials and methods

Chemicals

Sodium orthovanadate (Na_3VO_4), sodium β-glycerophosphate, sodium fluoride (NaF), dithiothreitol (DTT), and phenylmethylsulfonyl fluoride (PMSF) were purchased from Sigma Chemical Company (St. Louis, MO). Leupeptin, pepstatin, and aprotinin were purchased from Boehringer Mannheim (Indianapolis, IN). Iodoacetamide (an isopeptidase inhibitor) was obtained from Fluka Chemical Corp. (Milwaukee, WI). MG-132 and calpeptin were purchased from Calbiochem (La Jolla, CA). MG-132 and calpeptin were dissolved in dimethyl sulfoxide (DMSO) and stored at −80°C.

Cell culture and virus

Immortalized murine astrocytes (called C1 astrocytes) were maintained in Dulbecco's modified Eagle's medium (DMEM) supplemented with 10% fetal bovine serum (FBS; GIBCO) and antibiotics (100 units/ml penicillin and 100 μg/ml streptomycin) (Lin *et al*, 1997). All cells were grown at 37°C in a humidified incubator containing 5% CO_2. Cells were passaged biweekly and used for experimental purposes in the exponential growth phase. *ts*1, a spontaneous temperature-sensitive mutant of MoMuLV, was propagated in TB cells, a thymus-bone marrow cell line. Virus titers were determined by modified direct focus assay in 15F cells, a murine sarcoma-positive, leukemia-negative cell line, as previously described (Wong *et al*, 1981). For virus infection, C1 cells (4 × 105 cells) in DMEM containing 2% FBS and 4 μg/ml polybrene were seeded in 100-mm tissue culture dishes. After overnight culture, the medium was removed, and the cells were infected with *ts*1 virus at a multiplicity of infection (MOI) of 10 diluted in DMEM containing 2% FBS and 4 μg/ml polybrene and incubated for 1 h at 37°C under 5% CO_2. After virus adsorption, the medium containing virus was removed, DMEM containing 2% FBS was added to the culture, and the plates were incubated for various times at 38.5°C (Lin *et al*, 1997). For mock infection, C1 cells were treated identically, except that the medium used was DMEM containing polybrene only. For proteolysis inhibition study, either MG-132 (20 μM), calpeptin (20 μM), or DMSO only (less than 0.1%) was added to the culture medium of *ts*1- and mock-infected cells and the cells were incubated for an additional 4 h before cell lysate preparation. The concentrations of proteasome and calpain inhibitors were sufficient to inhibit IκBα and IκBβ proteolysis induced by various stimuli, such as TNF-α and LPS, as previously described (Miyamoto *et al*, 1998; Han *et al*, 1999).

Preparation of cell extracts

Whole cell extracts from C1 cells were prepared as follows. Briefly, cells were washed twice with cold phosphate-buffered saline (PBS, pH 7.4), and subsequently lysed with lysis buffer (50 mM Tris-HCl, pH 7.9, 150 mM NaCl, 1 mM ethylenediaminetetraacetic acid (EDTA), 1 mM Na_3VO_4, 30 mM β-glycerophosphate, 50 mM NaF, 10 mM iodoacetamide, 1 mM DTT, 1.0% NP-40, 1 mM PMSF, 10 μg/ml pepstatin, 10 μg/ml leupeptin, and 5 μg/ml aprotinin). After incubation on ice for 15 min, cell lysates were cleared by centrifugation at 13,000 × *g* for 20 min at 4°C. The supernatants were kept frozen at −80°C.

Nuclear and cytoplasmic extracts were prepared as described previously (Asin *et al*, 1999), with minor modifications. Cells were washed with cold PBS twice, gently scraped from the dishes, transferred to microcentrifuge tubes, and centrifuged for 10 minutes at 3,000 × *g*. The cells were resuspended in 5 pellet volumes of hypotonic buffer (10 mM HEPES, pH 7.9, 1.5 mM $MgCl_2$, 10 mM KCl, 1 mM EDTA, 1 mM Na_3VO_4, 30 mM β-glycerophosphate, 50 mM NaF, 10 mM iodoacetamide, 0.5 mM DTT, 0.1% NP-40, 1 mM PMSF, 10 μg/ml pepstatin, 10 μg/ml leupeptin, and 5 μg/ml aprotinin) and allowed to swell on ice for 15 min. The nuclei were then pelleted at 3,000 × *g* for 10 min at 4°C. The resulting cytoplasmic supernatants were transferred to fresh tubes and maintained on ice. The remaining pelleted nuclei were washed gently with hypotonic buffer and spun again, after which the supernatants were then discarded. Two pellet volumes of nuclear extraction buffer (20 mM HEPES, pH 7.9, 420 mM NaCl, 1.5 mM $MgCl_2$, 0.2 mM EDTA, 1 mM Na_3VO_4, 30 mM β-glycerophosphate, 50 mM NaF, 10 mM

iodoacetamide, 1 mM PMSF, 10 μg/ml pepstatin, 10 μg/ml leupeptin, and 5 μg/ml aprotinin) were added to nuclear pellets. Nuclear pellets were resuspended by vortexing, and the resulting nuclear lysates were maintained on ice for 20 min with occasional vortexing. All cytoplasmic and nuclear lysates were cleared by centrifugation at 13,000 × *g* for 20 min at 4°C, and all supernatants were kept frozen at −80°C. The protein content of the lysates was determined using the Bradford assay (Bio-Rad, Hercules, CA) and bovine serum albumin as the standard.

Western immunoblot analysis

Proteins (20 μg) were separated by 8–12% sodium dodecyl sulfate (SDS)-polyacrylamide gel electrophoresis (PAGE) and then transferred to nitrocellulose membranes (Schleicher and Schuell, Keene, NH). Kaleidoscope prestained standards (Bio-Rad) were used to determine molecular weights. The membranes were incubated for 1 h in blocking buffer (20 mM Tris-HCl-buffered saline containing 5% nonfat milk powder and 0.1% Tween 20) at room temperature. The membranes were probed with appropriate antibodies in 20 mM Tris-HCl-buffered saline containing 2% nonfat milk powder and 0.1% Tween 20 overnight at 4°C. Affinity-purified rabbit or goat polyclonal antibodies for RelA (p65) (SC-372), NF-κB (p50) (SC-1190), IκBα (SC-371), IκBβ (SC-945), cNOS (SC-1025), and iNOS (SC-650) were purchased from Santa Cruz Biotechnology (Santa Cruz, CA). A mouse monoclonal anti-β-actin antibody (A5441) was purchased from Sigma. The rabbit anti-ubiquitin antibody was generously provided by AL Haas (University of Wisconsin) (Haas and Bright, 1985). Normal rabbit IgG at the same dilutions was used as control. Blots were then incubated with anti-rabbit IgG-peroxidase conjugate (1 : 10,000 dilution; Kirkegaard Perry Laboratories, Gaithersburg, MD) and developed using the enhanced chemiluminesence (ECL) method (Amersham Life Science, Arlington Heights, IL). After stripping, the blots were then incubated with a mouse monoclonal anti-β-actin antibody to confirm equal protein leading and normalize the protein loading. Densitometric analysis of autoradiographs was performed by using a densitometer (Model GS-690, Bio-Rad) fitted with Multi-Analyst software (version 1.01; Bio-Rad).

Statistical analysis

Quantitative data obtained from the densitometric analysis of Western immunoblots were analyzed by paired *t*-test or analysis of variance (ANOVA). Statistical significance between groups was determined by Dunnett's multiple comparison analysis. *P* values <0.05 were considered statistically significant.

Acknowledgements

This work was supported in part by grants to PKY Wong from the NIH (A128283 and MH5718). We are grateful to Dr AL Haas (University of Wisconsin) for providing anti-ubiquitin antibody.

References

Akama KT, Albanese C, Pestell RG, Van Eldik LJ (1998). Amyloid beta-peptide stimulates nitric oxide production in astrocytes through an NFκB-dependent mechanism. *Proc Natl Acad Sci USA* **95:** 5795–5800.

Asin S, Taylor JA, Trushin S, Bren G, Paya CV (1999). Iκκ mediates NF-κB activation in human immunodeficiency virus-infected cells. *J Virol* **73:** 3893–3903.

Baeuerle PA, Baltimore D (1996). NF-κB: Ten years after. *Cell* **87:** 13–20.

Baldwin S (1996). The NF-κB and IκB proteins: New discoveries and insights. *Annu Rev Immunol* **14:** 649–683.

Beg AA, Baldwin AS (1993). The IκB proteins: Multifunctional regulators of Rel/NF-κB transcription factors. *Genes Dev* **7:** 2064–2070.

Benos DJ, Hahn BH, Bubien JK, Ghosh SK, Mashburn NA, Chaikin MA, Shaw GM, Benveniste EN (1994). Envelope glycoprotein gp 120 of human immunodeficiency virus type 1 alters ion transport in astrocytes: Implications for AIDS dementia complex. *Proc Natl Acad Sci USA* **91:** 494–498.

Bo L, Dawson TM, Wesselingh S, Mork S, Choi S, Kong PA, Hanley D, Trapp BD (1994). Induction of nitric oxide synthase in demyelinating regions of multiple sclerosis brains. *Ann Neurol* **36:** 778–786.

Borgland SL, Bowen GP, Wong NC, Libermann TA, Muruve DA (2000). A denovirus vector-induced expression of the C-X-C chemokine IP-10 is mediated through capsid-dependent activation of NF-κB. *J Virol* **74:** 3941–3947.

Chen Z, Hagler J, Palombella VJ, Melandri F, Scherer D, Ballard D, Maniatis T (1995). Signal-induced site-specific phosphorylation targets IκBα to the ubiquitin-proteasome pathway. *Genes Dev* **9:** 1586–1597.

Choe W, Stoica G, Lynn W, Wong PKY (1998). Neurodegeneration induced by MoMuLV-*ts*1 and increased expression of Fas and TNF-α in the central nervous system. *Brain Res* **779:** 1–8.

Crinelli R, Bianchi M, Gentilini L, Magnani M, Hiscott J (1999). Activation of the ubiquitin proteolytic system in murine acquired immunodeficiency syndrome affects IκBα turnover. *Eur J Biochem* **263:** 202–211.

Crinelli R, Fraternale A, Casabianca A, Magnani M (1997). Up-regulation of the ubiquitin-conjugating and proteolytic systems in murine acquired immunodeficiency syndrome. *Eur J Biochem* **247:** 91–97.

Cross AH, Manning PT, Keeling RM, Schmidt RE, Misko TP (1998). Peroxynitrite formation within the central nervous system in active multiple sclerosis. *J Neuroimmunol* **88:** 45–56.

DiDonato J, Mercurio F, Rosette C, Wu-Li J, Suyang H, Ghosh S, Karin M (1996). Mapping of the inducible IκB phosphorylation sites that signal its ubiquitination and degradation. *Mol Cell Biol* **16:** 1295–1304.

Dollard SC, James HJ, Sharer LR, Epstein LG, Gelbard HA, Dewhurst S (1995). Activation of nuclear factor κB in brains from children with HIV-1 encephalitis. *Neuropathol Appl Neurobiol* **21:** 518–528.

Gardner MB (1978). Type C viruses of wild mice: Characterization and natural history of amphotropic, ecotropic, and xenotropic MuLV. *Curr Top Microbiol Immunol* **79:** 215–259.

Good L, Sun SC (1996). Persistent activation of NF-κ B/Rel by human T-cell leukemia virus type 1 tax involves degradation of IκBβ. *J Virol* **70:** 2730–2735.

Haas AL, Bright PM (1985). The immunochemical detection and quantitation of intracellular ubiquitin-protein conjugates. *J Biol Chem* **260:** 12464–12673.

Han Y, Weinman S, Boldogh I, Walker RK, Brasier AR (1999). Tumor necrosis factor-α-inducible IκBα proteolysis mediated by cytosolic m-calpain. A mechanism parallel to the ubiquitin-proteasome pathway for nuclear factor-κb activation. *J Biol Chem* **274:** 787–794.

Hatakeyama S, Kitagawa M, Nakayama K, Shirane M, Matsumoto M, Hattori K, Higashi H, Nakano H, Okumura K, Onoe K, Good RA, Nakayama K (1999). Ubiquitin-dependent degradation of IκBα is mediated by a ubiquitin ligase Skp1/Cul 1/F-box protein FWD1. *Proc Natl Acad Sci USA* **96:** 3859–3863.

Jamaluddin M, Casola A, Garofalo RP, Han Y, Elliott T, Ogra PL, Brasier AR (1998). The major component of IκBα proteolysis occurs independently of the proteasome pathway in respiratory syncytial virus-infected pulmonary epithelial cells. *J Virol* **72:** 4849–4857.

Johnson DR, Douglas I, Jahnke A, Ghosh S, Pober JS (1996). A sustained reduction in IκB-β may contribute to persistent NF-κB activation in human endothelial cells. *J Biol Chem* **271:** 16317–16322.

Koprowski H, Zheng Y, Heber-Katz E, Fraser E, Rorke L, Fang F, Hanlon C, Dietzshold B (1993). *In vivo* expression of inducible nitric oxide synthase in experimentally induced neurologic diseases. *Proc Natl Acad Sci USA* **90:** 3024–3027.

Lee SC, Dickson DW, Liu W, Brosnan CF (1993). Induction of nitric oxide synthase activity in human astrocytes by interleukin-1 beta and interferon-gamma. *J Neuroimmunol* **46:** 19–24.

Lin YC, Chow CW, Yuen PH, Wong PKY (1997). Establishment and characterization of conditionally immortalized astrocytes to study their interaction with *ts*1, a neuropathogenic mutant of Moloney murine leukemia virus. *J NeuroVirol* **3:** 8–37.

Liou HC, Baltimore D (1993). Regulation of the NF-κ B/rel transcription factor and IκB inhibitor system. *Curr Opin Cell Biol* **5:** 77–487.

McKinsey TA, Brockman JA, Scherer DC, Al-Murrani SW, Green PL, Ballard DW (1996). Inactivation of IκBβ by the tax protein of human T-cell leukemia virus type 1: A potential mechanism for constitutive induction of NF-κB. *Mol Cell Biol* **16:** 2083–2090.

Miyamoto S, Seufzer BJ, Shumway SD (1998). Novel IκBα proteolytic pathway in WEHI231 immature B cells. *Mol Cell Biol* **18:** 19–29.

Pahl HL, Sester M, Burgert HG, Baeuerle PA (1996). Activation of transcription factor NF-κB by the adenovirus E3/19K protein requires its ER retention. *J Cell Biol* **132:** 511–522.

Pak J, Faller DV (1996). Moloney murine leukemia virus activates NF-κB. *J Virol* **70:** 4167–4172.

Patel A, Hanson J, McLean TI, Olgiate J, Hilton M, Miller WE, Bachenheimer SL (1998). Herpes simplex type 1 induction of persistent NF-κB nuclear translocation increases the efficiency of virus replication. *Virology* **247:** 212–222.

Peters RL, Spahn GJ, Rabstein LS, Kelloff GJ, Huebner RJ (1973). Murine C-type RNA virus from spontaneous neoplasms: *In vitro* host range and oncogenic potential. *Science* **181:** 665–667.

Rousset R, Desbois C, Bantignies F, Jalinot P (1996). Effects on NF-κB1/p105 processing of the interaction between the HTLV-1 transactivator Tax and the proteasome. *Nature* **381:** 328–331.

Shikova E, Lin YC, Saha K, Brooks BR, Wong PKY (1993). Correlation of specific virus-astrocyte interactions and cytopathic effects induced by *ts*1, a neurovirulent mutant of Moloney murine leukemia virus. *J Virol* **67:** 1137–1147.

Shirane M, Harumiya Y, Ishida N, Hirai A, Miyamoto C, Hatakeyama S, Nakayama K, Kitagawa M (1999). Down-regulation of p27(Kip 1) by two mechanisms, ubiquitin-mediated degradation and proteolytic processing. *J Biol Chem* **274:** 13886–13893.

Simmons M, Murphy S (1993). Cytokines regulate L-arginine-dependent cyclic GMP production in rat glial cells. *Eur J Neurosci* **5:** 825–831.

Sonenshein GE (1997). Rel/NF-κB transcription factors and the control of apoptosis. *Semin Cancer Biol* **8:** 113–119.

Sorimachi H, Ishiura S, Suzuki K (1997). Structure and physiological function of calpains. *Biochem J* **328:** 721–732.

Stoica G, Illanes O, Tasca SI, Wong PKY (1993). Temporal central and peripheral nervous system changes induced by a paralytogenic mutant of Moloney murine leukemia virus TB. *Lab Invest* **69:** 724–735.

Stoica G, Tasca SI, Wong PKY (2000). Motor neuronal loss and neurofilament-ubiquitin alteration in MoMuLV-*ts*1 encephalopathy. *Acta Neuropathol (Berl)* **99:** 238–244.

Szurek PF, Yuen PH, Ball JK, Wong PK (1990). A Val-25-to-Ile substitution in the envelope precursor polyprotein, gPr80env, is responsible for the temperature sensitivity, inefficient processing of gPr80env, and neurovirulence of *ts*1, a mutant of Moloney murine leukemia virus TB. *J Virol* **64:** 467–475.

Thompson JE, Phillips RJ, Erdjument-Bromage H, Tempst P, Ghosh S (1995). IκB-β regulates the persistent response in a biphasic activation of NF-κB. *Cell* **80:** 573–582.

Wong PKY, Floyd E, Szurek PF (1991). High susceptibility of FVB/N mice to the paralytic disease induced by *ts*1, a mutant of Moloney murine leukemia virus TB. *Virology* **180:** 365–371.

Wong PKY, Prasad G, Hansen J, Yuen PH (1989). *ts*1, a mutant of Moloney murine leukemia virus-TB, causes both

immunodeficiency and neurologic disorders in BALB/c mice. *Virology* **170:** 450–459.

Wong PKY, Soong MM, Yuen PH (1981). Replication of murine leukemia virus in heterologous cells: Interaction between ecotropic and xenotropic viruses. *Virology* **109:** 366–378.

Wu BY, Woffendin C, Duckett CS, Ohno T, Nabel GJ (1995). Regulation of human retroviral latency by the NF-κB/IκB family: Inhibition of human immunodeficiency virus replication by IκB through a Rev-dependent mechanism. *Proc Natl Acad Sci USA* **92:** 1480–1484.

Zandi E, Rothwarf DM, Delhase M, Hayakawa M, Karin M (1997). The IκB kinase complex (IKK) contains two kinase subunits, IKKα and IKKβ, necessary for IκB phosphorylation and NF-κB activation. *Cell* **91:** 243–252.